DOI: 10.1002/asia.201200723

Functionalization of Hexa-*peri*-hexabenzocoronenes: Investigation of the Substituent Effects on a Superbenzene

Ryuichi Yamaguchi,[a] Satoru Ito,[a] Byung Sun Lee,[b] Satoru Hiroto,[a] Dongho Kim,*[b] and Hiroshi Shinokubo*[a]

Abstract: We have demonstrated that the iridium-catalyzed direct borylation of hexa-*peri*-hexabenzocoronene (HBC) enables regioselective introduction of boryl groups to the *para*-, *ortho*-, and *meta*-substituted HBCs in high yields. The boryl groups have been transformed into various functionalities such as hydroxy, cyano, ethynyl, and amino groups. We have elucidated that the substituents significantly influence the photophysical properties of HBCs to enhance fluorescence quantum yields. DFT calculations revealed that the origin of the substituent effect is the lift in degeneracy in the frontier orbitals by an interaction with electron-donating and electron-withdrawing substituents at the *para*- and *ortho*-positions. The change in molecular orbitals results in an increase of the transition probability from the $S_0 \rightarrow S_1$ states. In addition, the two-photon absorption cross-section values of *para*-substituted HBCs are significantly larger than those of *ortho*- and *meta*-substituted HBCs.

Keywords: aromatic substitution · density functional calculations · hexa-*peri*-hexabenzocoronene · substituent effects · two-photon absorption

Introduction

Polycyclic aromatic hydrocarbons (PAHs) have been extensively investigated for their applications in electronic and optical molecular devices.[1–3] Their large π-conjugated planes not only enable efficient absorption of visible and near-infrared light but also facilitate the construction of a π–π stacking layer to allow significant intermolecular interactions, which are important in solid-state properties.[4] Among a large number of PAHs, hexa-*peri*-hexabenzocoronenes (HBCs) have been developed rapidly owing to the establishment of facile synthetic methods reported by Müllen and co-workers.[5]

Owing to the D_{6h} disk-like shape and the large π-conjugated plane, the HBC unit has often been employed as a building block for discotic liquid crystals.[6] However, with HBC molecules, the attention has been mainly focused on their properties in the aggregated state. A variety of HBCs have been synthesized to investigate their aggregation structures, which are deeply affected by the peripheral substituents.[7] Müllen and co-workers have reported trimethoxy-substituted HBCs, which form a helical packing layer in liquid crystalline mesophases.[7a] Recently, they have also reported HBCs with a large dipole moment induced by introducing cyano- and amino groups to the HBC core.[7c] On the other hand, the properties of non-aggregated HBC derivatives have remained unexplored. Although a number of functionalized HBCs have been synthesized, the dependence of the optical properties on the functional groups and their location has not been systematically investigated. As the HBC core can be regarded as a π-extended benzene, a so-called "superbenzene", studies on the substituent effects on a superbenzene should be important to understand the properties of HBCs at the molecular level.

We have investigated the substituent effects on the optical properties of functionalized HBCs. We anticipated that comparison of the optical properties of various substituted HBCs would reveal the substituent effects on the HBC core. To conduct this investigation, there were several structural considerations. To increase solubility and gain liquid crystalline mesophases, HBCs often possess long alkyl chains to induce facile aggregation,[8] which prevents thorough studies on the properties of the isolated HBC molecule. Accordingly, we anticipated that bulky substituents would be preferable for investigating the optical properties of HBCs.[9] Although *tert*-butyl-substituted HBCs have been synthesized, their solubility was very limited.[10] We have recently reported the synthesis of mesityl-substituted HBCs through Kumada–Tamao–Corriu cross-coupling reactions.[11] These compounds were fairly soluble in common organic solvents and seemed to be optimal substrates for investigations on HBCs in the non-aggregated state.

[a] R. Yamaguchi, S. Ito, Dr. S. Hiroto, Prof. Dr. H. Shinokubo
Department of Applied Chemistry, Graduate School of Engineering, Nagoya University, Aichi, 464-8603 (Japan)
Fax: (+81) 52-789-3188
E-mail: hshino@apchem.nagoya-u.ac.jp

[b] B. S. Lee, Prof. Dr. D. Kim
Department of Chemistry, Yonsei University
Seoul 120-749 (Korea)
Fax: (+82) 2-2123-2434
E-mail: dongho@yonsei.ac.kr

Supporting information for this article is available on the WWW under http://dx.doi.org/10.1002/asia.201200273.

To install various functionalities to HBCs, we employed the direct C–H borylation, which has proven to be a reliable tool for introduction of boryl groups to functionalized π-systems.[12] A couple of examples of iridium-catalyzed borylation reactions toward PAHs have been reported.[13] For example, Marder and co-workers have reported that direct borylation of pyrenes occurs at the 2,7-positions, thereby enabling facile preparation of 2,7-substituted pyrenes, which are not easily accessible by conventional electrophilic substitution reactions.[13f] We have also developed an iridium-catalyzed direct borylation of perylene bisimides and mesityl-substituted HBCs.[11] The resulting borylated products are useful intermediates for further transformations such as Suzuki–Miyaura coupling and oxidation reactions. After construction of the HBC core, it can be functionalized to synthesize various HBC derivatives by using the rich chemistry of organoboron reagents.

Herein we disclose synthetic methods for the functionalization of various HBCs through borylated HBCs. In addition, the effect of the substituents on the optical properties—depending on the position of the functionality—is discussed on the basis of the DFT calculations. In this study, we employed three types of HBCs **1a**, **1b**, and **1c** as starting materials. These substrates are *para*-, *ortho*-, and *meta*-substituted HBCs, respectively, in analogy with substituted benzene derivatives.

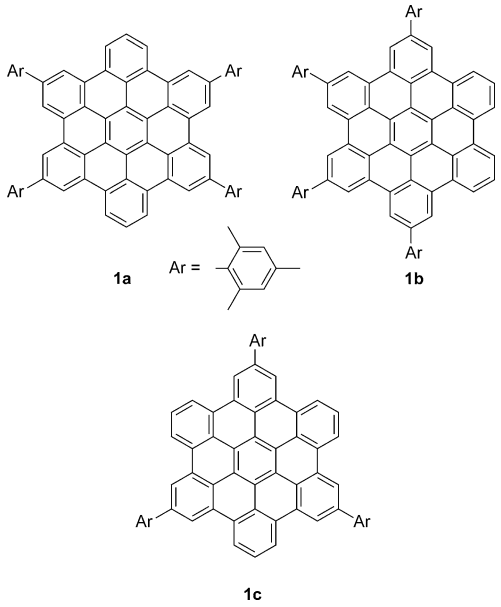

Abstract in Japanese:

パラ、オルト、メタ位にメシチル基をもつヘキサペンゾコロネン(HBC)のイリジウム触媒による位置選択的な直接ホウ素化に成功した。ボリル基は、ヒドロキシ基、シアノ基、エチニル基、アミノ基といった様々な官能基に変換することができた。さらに、蛍光量子収率がパラ位またはオルト位に置換基を導入した場合に増大することを見いだした。これは、パラ位またはオルト位の電子供与基または電子求引基との相互作用によって、HBC のフロンティア軌道の縮退が解けることが原因であることを DFT 計算により明らかにした。さらに、パラ位に官能基をもつ HBC の二光子吸収断面積の値が、オルト、メタ置換体に比べて大きいことを明らかにした。

Results and Discussion

Iridium-Catalyzed Direct Borylation of HBCs and Oxidation

Iridium-catalyzed direct borylation of **1a** and **1c** has already been reported in our previous study.[11] The direct borylation of **1b** was performed with [{Ir(OMe)(cod)}$_2$] (cod = cycloocta-1,5-diene), 4,4′-di-*tert*-butyl-2,2′-bipyridyl (dtbpy), and 4.0 equivalents of bis(pinacolate)diboron (B_2pin_2) in a mixture of mesitylene and *tert*-butyl methyl ether (2:1 (v/v)) at reflux for 36 h to provide diborylated product **2b** in 88% yield (Scheme 1). Diborylated HBCs **2a** and **2c** were easily converted into their corresponding dihydroxy-substituted HBCs **3a** and **3c** in high yields by using H_2O_2 as an oxidant. On the other hand, *ortho*-substituted HBC **2b** decomposed upon oxidation under the same reaction conditions. In this case, we found that 4.0 equivalents of Oxone oxidized **2b** effectively into the dihydroxy HBC **3b** in 79% yield. The structure of **3b** was unambiguously confirmed by X-ray diffraction analysis.[14] As shown in Figure 1, two hydroxy groups were placed at the *ortho*-position of the HBC periphery. In sharp contrast to **3a** and **3c**, which exhibit a non-stacked structure induced by hydrogen-bonding interactions between hydroxy groups, **3b** forms π–π stacking columnar structures in the crystal. The distances between the two closest HBC molecules are 3.35 and 3.25 Å, which are much shorter than the sum of the van der Waals radii of carbon atoms. The HBC core was slightly distorted and the mean plane deviation was 0.127 Å. The distortion may be caused by a crystal packing interaction. The difference in packing among the three types of HBCs **3a**, **3b**, and **3c** is probably related to the presence of π–π interactions. For only *ortho*-substituted HBC **3b**, enough of the HBC π-surface area is available to interact with the other molecule, thereby allowing a columnar packing structure.

Preparation of *para*-, *meta*-, and *ortho*-Substituted HBCs with Electron-Donating and Electron-Withdrawing Groups

Scheme 2 describes various functionalizations of *para*-substituted HBC **3a**. Methoxy-substituted HBC **5a** was readily prepared in 89% yield upon treatment of **3a** with an excess amount of methyl iodide under basic conditions in a mixture of refluxing tetrahydrofuran (THF)/acetone (3:1, v/v).[15] Other substituents were introduced through transition-metal catalyzed processes. As halogenation of borylated HBCs with $CuBr_2$ or NaI and chloramine-T gave poor results,[16] we prepared the triflate **4a** from **3a** for palladium-catalyzed reactions. Bistriflate **4a** was obtained in 86% yield in one step by using 4.0 equivalents of Tf_2O and pyridine. Sonogashira coupling of **4a** with 3,3-dimethyl-1-propyne afforded **6a** in 97% yield in the presence of [$PdCl_2(PPh_3)_2$] (3 mol%), CuI (6 mol%), and 1,8-diazabicyclo[5.4.0]undec-7-ene (DBU; 6.0 equiv). Under the same reaction conditions, alkynyl-substituted HBCs **6b** and **6c** were prepared in 85% and 97% yield, respectively. Introduction of amino groups was achieved through a Buchwald–Hartwig amina-

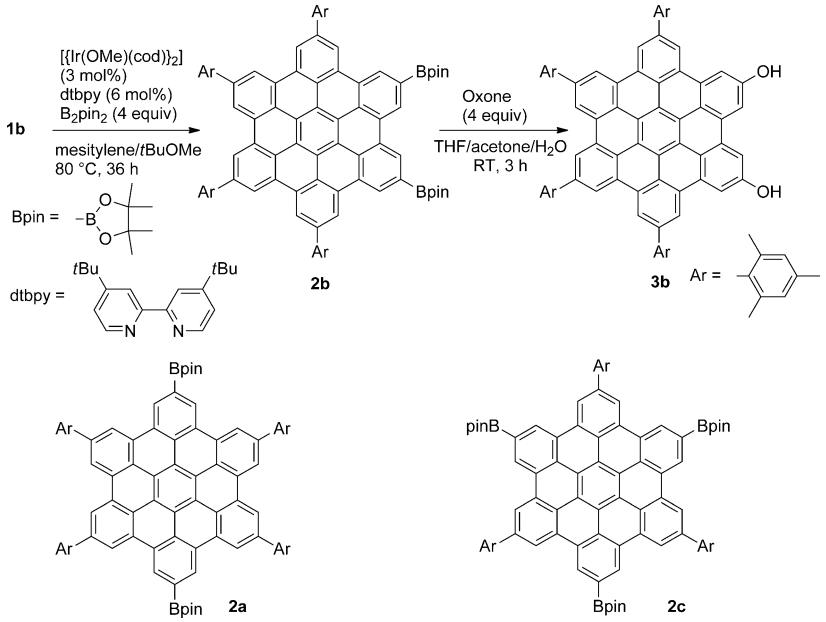

Scheme 1. Iridium-catalyzed borylation of **1b** and oxidation of **2b**.

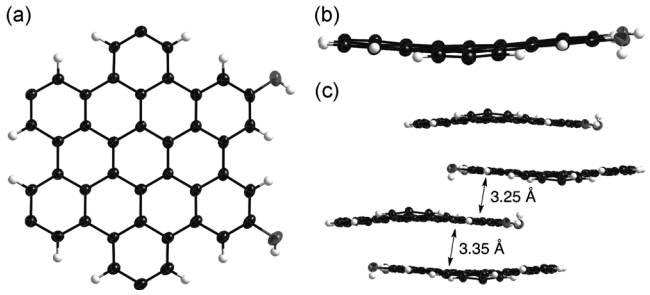

Figure 1. X-ray structure of **3b**. a) Top view, b) side view, and c) crystal packing. The thermal ellipsoids are scaled at 50% probability level. Mesityl groups are omitted for clarity.

tion.[17] In our first trial, however, the reaction of **4a** with mesitylamine in the presence of $[Pd_2(dba)_3]\cdot CHCl_3$, tri(*tert*-butyl)phosphine, and sodium *tert*-butoxide provided only the hydrolyzed product **3a** in 82% yield. After several trials, 1,1′-diphenylphosphinoferrocene (DPPF) was found to be effective to afford diamino HBC **7a** in 16% yield. By using Cs_2CO_3 as a base greatly improved the yield of **7a** to 86% yield. By following the same procedure, *ortho*-diamino HBC **7b** was also synthesized in 86% yield (Scheme 3). Introduction of cyano substituents was carried out by using Takagi's cyanation protocol with 8.0 equivalents of KCN in the presence of zinc powder and a catalytic amount of $[Pd_2(dba)_3]\cdot CHCl_3$ and DPPF.[18] Owing to the low solubility of **4a** in *N*-methylpyrollidone (NMP), the reaction was performed in a mixed solvent system. The reaction in toluene/NMP produced dicyano-substituted **8a** in 72% yield. Under the same reaction conditions, cyano-substituted HBCs **8b** and **8c** were also prepared in 72% and 52% yield, respectively (see Schemes 3 and 4). Notably, the addition of a catalytic amount of zinc powder dramatically improved the yield of the cyanation products and no reaction occurred in the absence of zinc. Unfortunately, trimethoxy- and triamino-substituted products from the *meta*-substituted HBC could not be isolated owing to their instability under aerobic conditions. All of the obtained products were fully characterized by NMR and mass spectroscopic analysis.

Photophysical Properties

Although a number of functionalized HBCs have been reported, there have been rather few studies on their photophysical properties, in particular, fluorescence spectra of HBCs in the non-aggregated state. Owing to the bulky mesityl groups that avoid formation of the excimer, the present HBC derivatives are suitable to investigate their unimolecular photophysical properties. Figure 2a shows the UV/Vis absorption spectra of the series of *para*-substituted HBCs in CH_2Cl_2. Müllen and co-workers have reported that an electronic absorption spectrum of HBC derivatives usually consists of three representative absorption bands, α-, β-, and *p*-bands.[19] The α-band is the lowest energy band, which has usually low intensity owing to its forbidden nature of the $S_0 \rightarrow S_1$ transition. As shown in Figure 2a, the α-band is strongly affected by the substituents. In comparison to **1a**, all *para*-substituted HBCs showed bathochromic shifts of the α-bands, thus indicating their narrower HOMO–LUMO gaps. In particular, **7a** showed the longest bathochromic shift of the α-band at 491 nm. In addition, intense α-bands were observed for **6a**, **7a**, and **8a**. Among them, the amino-substituted HBC **7a** shows the largest α-band ($\varepsilon = 14\,000\ cm^{-1}M^{-1}$), and this implies that the π-donating nature of amino groups significantly influences the transition probability of the α-band. Figure 2b shows UV/Vis absorption spectra of *ortho*-substituted HBCs in CH_2Cl_2. A similar trend of the substituent effect on the α-bands was observed. As compared to *para*-substituted HBCs, broadened spectra were observed because of their less symmetrical nature. The degree of the bathochromic shift and enhancement in the α-bands was smaller than that for *para*-substituted HBCs. Only **7b** exhibited an intense α-band at 486 nm with an extinction coefficient of $\varepsilon = 7900\ cm^{-1}M^{-1}$. This result indicates that the substituent effects at the *ortho*-position of the HBC core are weaker than those at the *para*-position. Figure 2c shows UV/Vis absorption spectra of *meta*-substituted HBCs **1c**, **6c**, and **8c** in CH_2Cl_2. Although *meta*-substituted HBCs have an additional substituent on the HBC core, compared to *para*- and *ortho*-substituted HBC, the spectra of all the

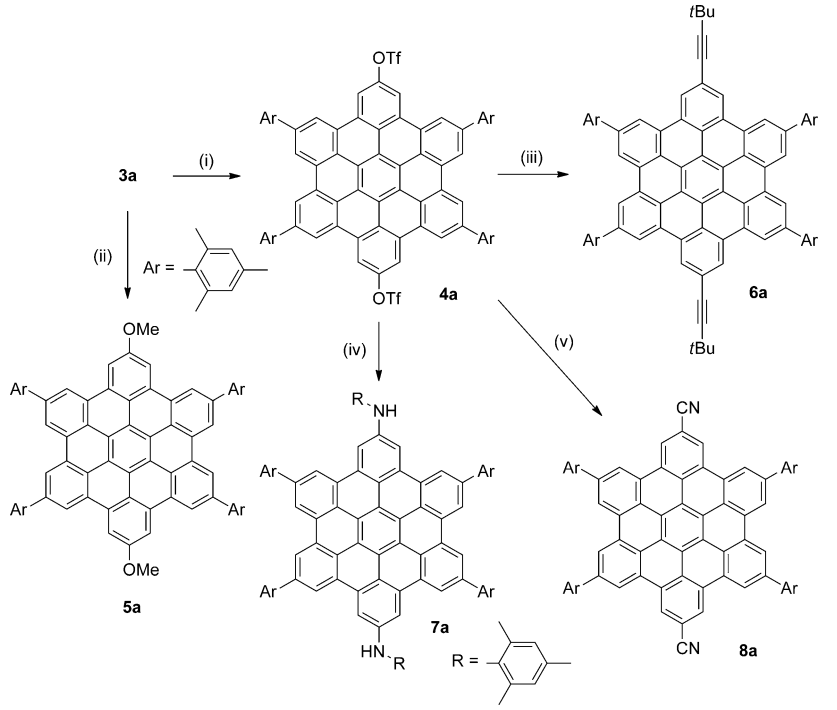

Scheme 2. Introduction of various functionalities to *para*-substituted HBC **1a**. Reagents and conditions: (i) Tf_2O (4.0 equiv), pyridine (8.0 equiv), CH_2Cl_2, rt, 3 h; (ii) MeI (excess), K_2CO_3 (8.0 equiv), THF/acetone = 3:1, reflux, 24 h; (iii) 3,3-dimethyl-1-butyne (4.0 equiv), $[PdCl_2(PPh_3)_2]$ (3 mol%), CuI (6 mol%), DBU (6.0 equiv), THF, rt, 18 h; (iv) 2,4,6-trimethylaniline (8.0 equiv), $[Pd_2dba_3]\cdot CHCl_3$ (5 mol%), DPPF (10 mol%), Cs_2CO_3 (6.0 equiv), toluene, reflux, 30 h; (v) KCN (8.0 equiv), $[Pd_2dba_3]\cdot CHCl_3$ (5 mol%), DPPF (10 mol%), Zn (6 mol%), toluene/NMP = 1:1, 60 °C, 24 h.

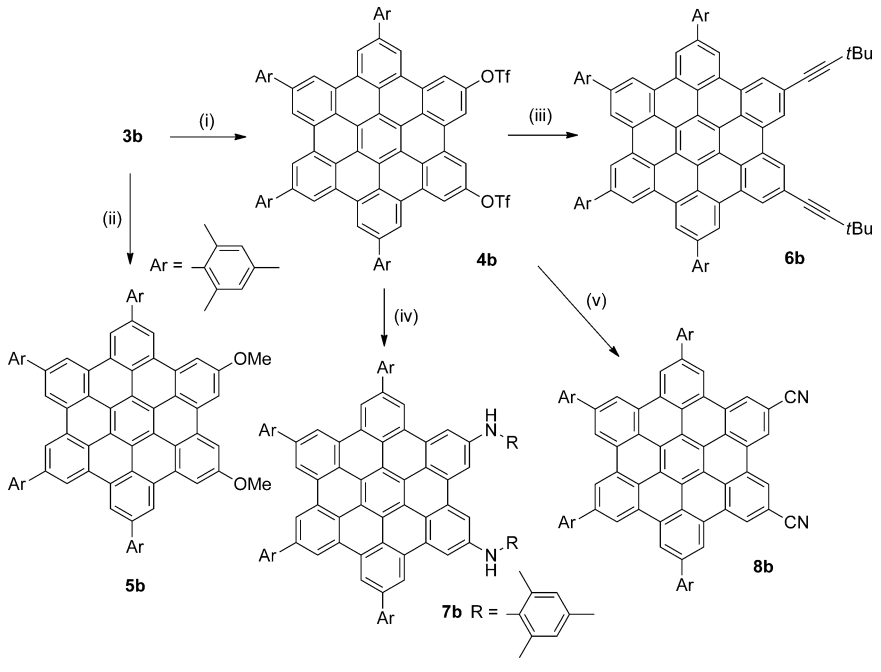

Scheme 3. Introduction of various functionalities to *ortho*-disubstituted HBC **1b.** Reagents and conditions: (i) Tf_2O (4.0 equiv), pyridine (8.0 equiv), CH_2Cl_2, rt, 3 h; (ii) MeI (excess), K_2CO_3 (6.0 equiv), THF/acetone = 3:1, reflux, 24 h; (iii) 3,3-dimethyl-1-butyne (4.0 equiv), $[PdCl_2(PPh_3)_2]$ (3 mol%), CuI (6 mol%), DBU (6.0 equiv), THF, rt, 18 h; (iv) 2,4,6-trimethylaniline (8.0 equiv), $[Pd_2dba_3]\cdot CHCl_3$ (5 mol%), BINAP (10 mol%), Cs_2CO_3 (6.0 equiv), toluene, reflux, 24 h; (v) KCN (8.0 equiv), $[Pd_2dba_3]\cdot CHCl_3$ (3 mol%), DPPF (6 mol%), Zn (6 mol%), toluene/NMP = 1:1, 100 °C, 24 h.

meta-substituted HBCs did not show any changes. In particular, the α-bands appeared with quite low intensity, thus suggesting that the substituents at the *meta*-positions have a negligible effect on the electronic structure of the HBC core.

Figure 3 shows emission spectra of *para*-, *ortho*-, and *meta*-substituted HBCs in CH_2Cl_2. The shape of the fluorescence spectra of **5a** is similar to that of **1a**; this displays fine vibronic structures. For either electron-donating or electron-withdrawing substituents, the vibronic structures became broadened to show three obvious bands that are attributed to (0-0), (0-1), and (0-2) vibronic transitions for *para*-, *ortho*-, and *meta*-substituted HBCs, respectively. The substituents also influence the fluorescence quantum yields. HBC **1a** exhibited fluorescence with a low quantum yield ($\Phi = 0.028$). Introduction of alkynyl substituents does not have much influence on the quantum yield ($\Phi = 0.033$). On the other hand, both electron-donating and electron-withdrawing substituents enhance the quantum yields to above 0.10. Amino-substituted HBC **7a** showed the highest quantum yield ($\Phi = 0.33$) among the HBCs that we have prepared. These observed quantum yields seem to be related with the intensity of the α-bands. Namely, HBCs with a more allowed $S_0 \rightarrow S_1$ transition have higher fluorescence quantum yields. A similar trend was also observed for *ortho*-substituted HBCs, but *ortho*-substituted HBCs show a smaller enhancement in the fluorescence quantum yields than those of *para*-substituted HBCs: The quantum yield of **7b** is only $\Phi = 0.20$, which is about a half the value of **7a**. For *meta*-substituted HBCs, an

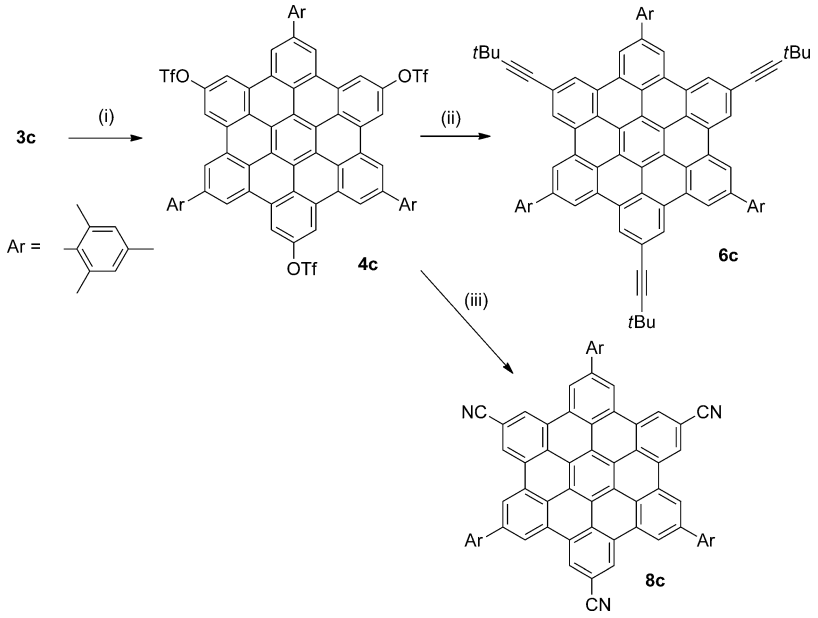

Scheme 4. Introduction of various functionalities to *meta*-substituted HBC **1c.** Reagents and conditions: (i) Tf_2O (6.0 equiv), pyridine (8.0 equiv), CH_2Cl_2, rt, 16 h; (ii) 3,3-dimethyl-1-butyne (6.0 equiv), $[PdCl_2(PPh_3)_2]$ (5 mol%), CuI (10 mol%), DBU (6.0 equiv), THF, rt, 24 h; (iii) KCN (12.0 equiv), $[Pd_2dba_3]\cdot CHCl_3$ (5 mol%), DPPF (10 mol%), Zn (6 mol%), toluene/NMP = 1:1, 60 °C, 24 h.

enhancement in the fluorescence quantum yields with substituents was not observed. A fine vibronic structure was observed for cyano-substituted **8c**, while both **8a** and **8b** showed a rather broad spectrum. These spectroscopic studies clearly demonstrate that the substituent effect on the HBC core increases in the order of *meta*-, *ortho*-, and *para*-substituted HBCs.

Theoretical Investigations

We then performed theoretical calculations on several HBCs to elucidate the substituent effect on the optical properties of HBCs. Peripheral mesityl and *N*-mesityl groups were replaced with hydrogen atoms and methyl groups, respectively, to reduce the calculation cost. The molecular geometries were fully optimized by the density-functional theory (DFT) based on B3LYP hybrid functional with the 6–31G(d) basis set.[20] Oscillator strengths were calculated by the time-dependent DFT (TD-DFT) method.

Figure 4 displays the calculated frontier orbitals and energy diagrams. Unsubstituted HBC **I** has two sets of degenerate frontier orbitals, HOMO and HOMO-1 as well as LUMO and LUMO+1 (Figure 4a). As reported by Müllen and co-workers, both the α-band and β-band result from the transitions between these two degenerated HOMOs and LUMOs. The forbidden feature of the α-band is due to the configuration interaction of these degenerate transitions (Table 1, entry 1).[21]

Figure 4b shows the energy diagrams of *para*- and *ortho*-diamino HBCs **II-a** and **II-b** as well as the parent HBC **I**. For both diamino-substituted HBCs, the introduction of amino groups destabilizes one of two HOMOs, thereby resulting in splitting of the degenerated orbitals. The removal of degeneracy can be explained by the interaction of two HOMOs of the parent HBC with the amino groups. One HOMO interacts significantly with the electron-donating amino groups to destabilize the energy level, while the other stays at almost the same energy level owing to the lack of an interaction at the nodal plane position of the molecular orbital. As a result, the two orbitals have different energies. This situation can be confirmed from the molecular orbitals of diamino HBCs. Figure 5 illustrates the HOMO and HOMO-1 of *para*-diamino HBC **II-a**, in which the HOMO has a substantial contribution from the amino groups, while the HOMO-1 has no molecular orbital coefficient on the nitrogen atoms.

The splitting of HOMO and HOMO-1 weakened the configuration interaction to enhance the oscillator strengths of the α-bands (Table 1, entries 2 and 3). The higher oscillator strength would lead to the higher radiative rate constant because of the rigid structure of the HBC unit. The observed fluorescence quantum yield of the amino-substituted HBCs was substantially higher than the unsubstituted HBC. Accordingly, the splitting of HOMO and HOMO-1 should be related to the enhancement in emission efficiency in amino-substituted HBCs **8a** and **8b**.

Figure 4c shows the energy diagrams of cyano HBCs **III-a**, **III-b**, and **III-c**. In comparison to unsubstituted HBCs, dicyano HBCs **III-a** and **III-b** have LUMO and LUMO+1 of different energies, while HOMO and HOMO-1 are almost degenerate. For tricyano HBC **III-c**, both HOMOs and LUMOs are almost degenerate as well as the parent HBC.

In the case of *para*-dicyano-substituted HBC **III-a**, the substituent interacts with the LUMO but not with LUMO+1 (Figure 6). One of the two degenerate LUMOs is stabilized by effective hybridization with the electron-withdrawing cyano groups, thereby resulting in the splitting of LUMO and LUMO+1.

Compared to the amino-substituted HBCs, the oscillator strengths of the α-band for the cyano-substituted HBCs are relatively small (Table 1, entry 4–6). In addition, the oscillator strengths decrease in the order of *para*, *ortho*, and *meta*. This order is the same as that of the energy gaps between LUMO and LUMO+1. This result suggests that the degree of the splitting in the LUMOs is responsible for the oscillator strength of the α-band of cyano HBCs. In *meta*-cyano substituted HBC **III-c**, which has almost degenerate

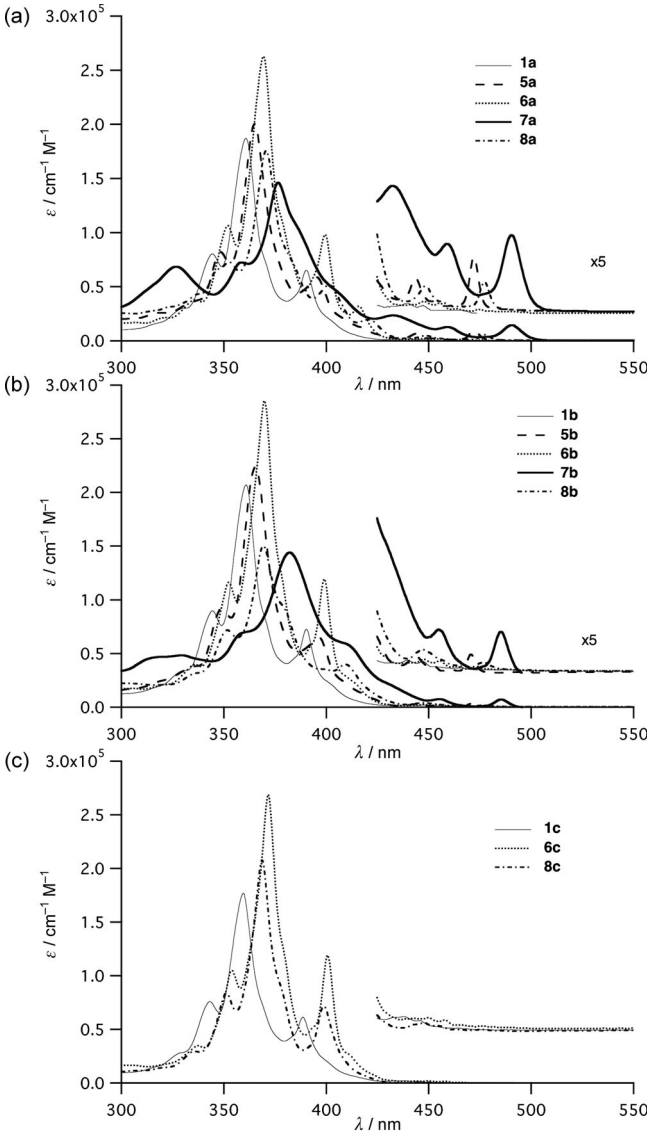

Figure 2. UV/Vis absorption spectra of a) *para*-disubstituted HBCs **1a**, **5a**, **6a**, **7a**, and **8a**, b) *ortho*-disubstituted HBCs **1b**, **5b**, **6b**, **7b**, and **8b**, and c) *meta*-disubstituted HBCs **1c**, **6c**, and **8c**. All spectra were recorded at 3.0×10^{-6} M in dichloromethane.

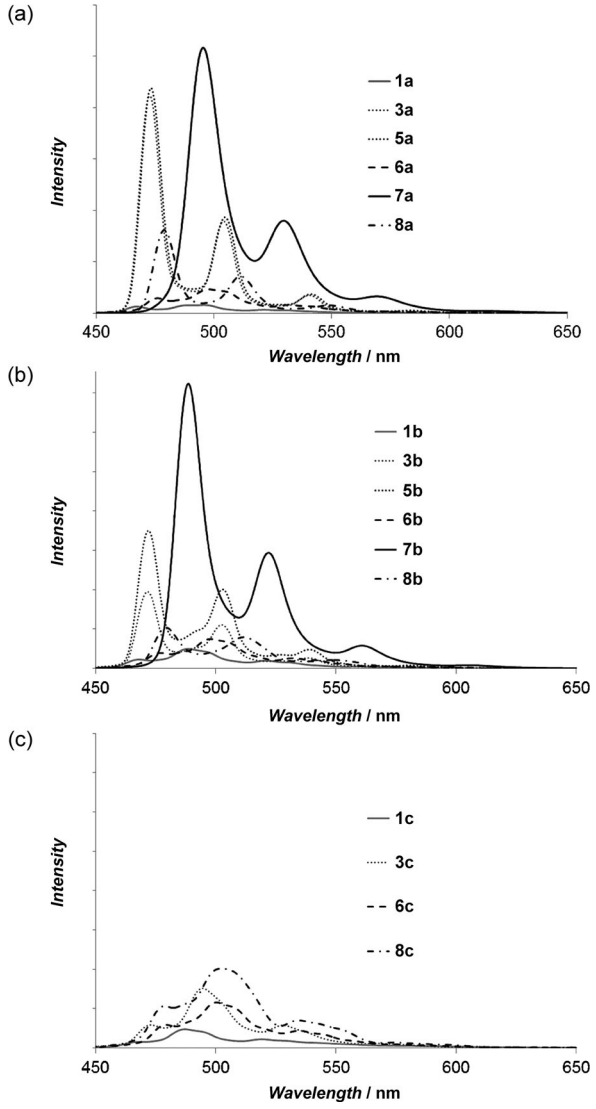

Figure 3. Emission spectra of a) *para*-disubstituted HBCs **1a**, **3a**, **5a**, **6a**, **7a**, and **8a**, b) *ortho*-disubstituted HBCs **1b**, **3b**, **5b**, **6b**, **7b**, and **8b**, and c) *meta*-disubstituted HBCs **1c**, **3c**, **6c**, and **8c**. All spectra were recorded at 2.0×10^{-6} M in dichloromethane with excitation at 400 nm.

LUMOs, transition of the lowest energy band is completely forbidden.

The oscillator strengths of the α-band by TD-DFT calculations and observed fluorescence quantum yields of substituted HBCs are plotted in Figure 7. Interestingly, an almost linear and positive correlation was obtained. This result indicates that the oscillator strength of the α-band is critical to the fluorescence quantum yield of substituted HBCs. The substituents at the *para*- and *ortho*-positions effectively lift the degeneracy of the HOMOs or LUMOs to enhance the oscillator strengths of the lowest energy band, thus affording higher fluorescence quantum yields.

Non-Linear Optical Studies

As HBCs have rigid and large π-conjugated planes, they have been attractive targets for materials with large two-photon absorption (TPA) cross-section values. Recently, Wu and co-workers synthesized octupolar HBCs that bear donors and acceptors at the HBC periphery, thus exhibiting large TPA cross sections.[22] Encouraged by this result, we investigated the TPA cross-section of three-types of substituted HBCs to clarify the regiochemical dependence of the non-linear optical (NLO) properties. The results are summarized in Table 2 and Figure S43 (see the Supporting Information). The TPA cross-section values were measured at 800 nm in toluene. Among three alkynyl-substituted HBCs, **6a** had the largest TPA cross-section value (700 GM), while **6b** and **6c** showed lower values (400 and 480 GM, respectively). The larger value for *para*-substituted HBC **6a** is

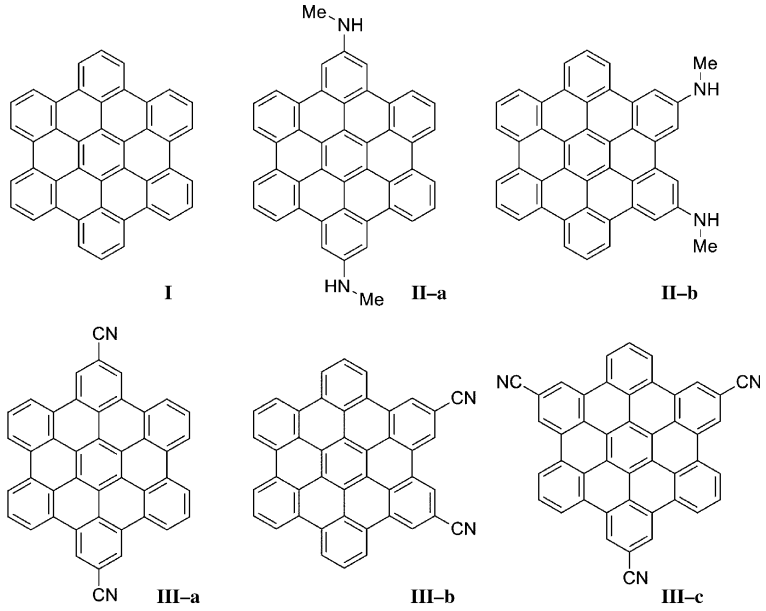

I II–a II–b III–a III–b III–c

probably due to effective conjugation over the HBC plane compared to *ortho*- and *meta*-substituted HBCs. This result is consistent with those obtained by single-photon optical analysis. The same trend was also observed for another series of HBCs. *para*-Substituted HBC **7a** had a larger TPA cross-section value of 910 GM than that of *ortho*-substituted HBC **7b** (440 GM). Due to the instability of the *meta*-amino-substituted HBC under aerobic conditions, we could not measure its TPA cross-section value. With regard to the NLO properties, large molecular polarizability is an important factor to contribute to a large TPA cross-section value. Many efforts have been directed for enhancing the TPA cross-section value by using a donor (D)/acceptor (A)-type chromophoric system, introducing additional groups to perturb the charge redistribution. In terms of the effect of various functional groups on NLO properties, the introduction of amino groups (D) to HBCs is more effective than those of cyano groups (A). We can conclude that the NLO properties of HBCs were dependent on the introduction of functional groups and their locations.

Conclusions

In conclusion, we have demonstrated the introduction of various functional groups after construction of the HBC skeleton through iridium-catalyzed C–H borylation. Three types of HBCs, *para*-, *meta*-, and *ortho*-substituted HBCs, could be readily prepared in high yields through transition-metal catalyzed transformation of HBC bistriflates. The electron-donating and electron-accepting groups substantially alter electronic structures of HBCs, thus showing bathochromic shifts in their absorption and emission spectra. In particular, introduction of amino and cyano groups intensified the α-bands of the absorption spectra and enhanced fluorescence quantum yields of HBCs. Importantly, the effect of the substituents significantly depends on their location: *para*-disubstituted HBCs experience the largest substituent effects than other HBCs. According to the theoretical analysis, the enhanced α-bands can be accounted for by the splitting of degenerate HOMOs with electron-donating substituents or LUMOs with electron-accepting groups. Interestingly, the fluorescence quantum yields show a linear correlation with oscillator strengths of the α-bands. These results demonstrate that the emission properties of HBCs can be manipulated by electron-donating and electron-accepting groups at the appropriate positions. The present strategy for functionalization of HBCs should be useful for development in the field of PAHs. The potential application of the present substituted HBCs for electronic devices is currently under investigation.

Experimental Section

Instrumentation and Materials

^{1}H NMR (500 MHz) and ^{13}C NMR (126 MHz) spectra were recorded on a Varian INOVA-500 spectrometer, and chemical shifts were reported in ppm relative to $CHCl_3$ ($\delta = 7.260$ ppm) for ^{1}H NMR and $CDCl_3$ ($\delta = 77.0$ ppm) for ^{13}C NMR. UV/Vis absorption spectra were recorded on a Shimadzu UV-2550 or JASCO V670 spectrometer. Emission spectra were recorded on a JASCO FP-6500 spectrometer and absolute fluorescence quantum yields were measured by a photon-counting method using an integration sphere. Mass spectra were recorded on a Bruker micro-TOF using a ESI-TOF method in the positive and negative mode for acetonitrile solutions. X-ray data were recorded on a Bruker SMART APEX X-Ray diffractometer equipped with a large area CCD detector. Unless otherwise noted, materials obtained from commercial suppliers were used without further purification.

*5,8,14,17-Tetramesitylhexabenzo[bc,ef,hi,kl,no,qr]coronene-2,11-diyl bis(trifluoromethanesulfonate) (**4a**)*

A flask containing **3a** (616 mg, 0.6 mmol) was purged with N_2, and then charged with anhydrous and degassed CH_2Cl_2 (8 mL) and pyridine (0.39 mL, 8.0 equiv). Then the mixture was stirred for 1 min. Trifluoromethanesulfonic anhydride (0.41 mL, 4.0 equiv) was added to this mixture dropwise at room temperature. The mixture was then stirred at room temperature for 3 h, quenched with aqueous HCl (1 M), extracted with CH_2Cl_2, and then dried over Na_2SO_4. The solvents were removed under vacuum, and the crude product was purified by silica-gel column chromatography (CH_2Cl_2/*n*-hexane = 1:2) and recrystallized from CH_2Cl_2/MeOH to afford **4a** (667 mg, 0.52 mmol) in 86% yield as a yellow solid. ^{1}H NMR ($CDCl_3$, 500 MHz): $\delta = 9.11$ (s, 4H), 9.03 (s, 4H), 9.02 (s, 4H), 7.16 (s, 8H), 2.47 (s, 12H), 2.25 ppm (s, 24H); ^{13}C NMR ($CDCl_3$, 126 MHz): $\delta = 148.9$, 140.8, 138.5, 137.7, 136.2, 133.4, 130.9, 129.8, 128.6, 125.1, 124.9, 124.9, 124.6, 124.0, 121.5, 120.9, 114.7, 21.3, 21.2 ppm; UV/

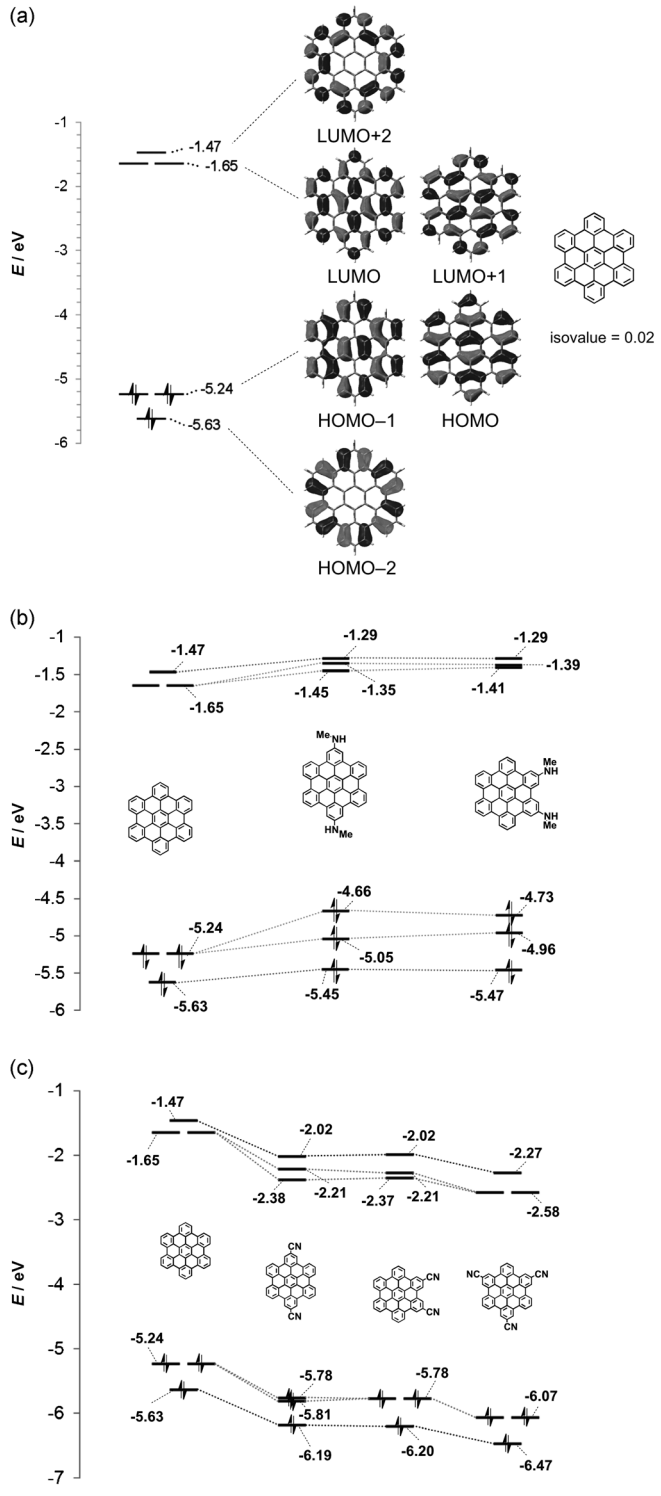

Figure 4. Energy diagrams of the HBC derivatives. a) Unsubstituted HBC, b) *para*- and *ortho*-diamino HBCs, and c) *para*-dicyano, *ortho*-dicyano, and *meta*-tricyano HBCs.

Vis (CH_2Cl_2): λ_{max} (ε [$M^{-1}cm^{-1}$]) = 347 (93000), 363 (220000), 393 nm (75000); HR-MS (ESI-MS): m/z = 1291.3446, calcd for $(C_{80}H_{56}F_6O_6S_2)^+$ = 1291.3495 [$(M+H)^+$].

Table 1. Calculated wavelengths and oscillator strengths of α-bands of HBC derivatives by the TD-DFT method.

Entry	Compounds	Excitation wavelength [nm]	Excited state	CI coefficient	Oscillator strength, *f*
1	**I**	428	HOMO-1→LUMO HOMO→LUMO+1	0.50537 0.50532	0
		409	HOMO-1→LUMO+1 HOMO→LUMO	-0.49275 0.49464	0
2	**II-a**	454	HOMO-1→LUMO+1 HOMO→LUMO	0.32398 0.61536	0.0580
		435	HOMO-1→LUMO HOMO→LUMO+1	-0.32185 0.61147	0.0923
3	**II-b**	447	HOMO-1→LUMO+1 HOMO→LUMO	-0.39932 0.58068	0.0267
		432	HOMO-1→LUMO HOMO→LUMO+1	0.37928 0.58068	0.0467
4	**III-a**	440	HOMO→LUMO HOMO→LUMO+1	0.54725 -0.44042	0.0055
		424	HOMO-1→LUMO+1 HOMO→LUMO	0.37462 0.59718	0.0584
5	**III-b**	442	HOMO-1→LUMO+1 HOMO→LUMO	-0.4718 0.52311	0.0022
		426	HOMO-1→LUMO HOMO→LUMO+1	0.50797 0.48404	0.0066
6	**III-c**	441	HOMO-1→LUMO HOMO→LUMO+1	0.49753 0.49627	0
		422	HOMO-1→LUMO HOMO→LUMO+1	-0.49602 0.50115	0

*2,5,11,14-Tetramesityl-8,17-dimethoxyhexabenzo[bc,ef,hi,kl,no,qr]coronene (**5a**)*

A flask containing **3a** (20.5 mg, 0.02 mmol) and potassium carbonate (22.1 mg, 8.0 equiv) was purged with N_2, and then charged with an anhydrous and degassed mixture of THF/acetone = 3:1 (4 mL). Iodomethane (0.4 mL, excess) was added dropwise to this mixture at room temperature. The mixture was then stirred under reflux for 24 h, quenched with aqueous HCl (1 M), extracted with CH_2Cl_2, and then dried over Na_2SO_4.

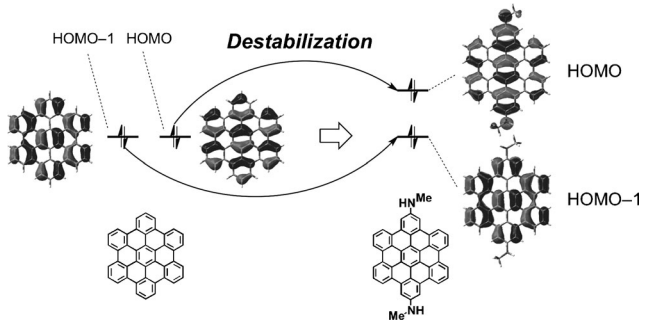

Figure 5. Removal of the degeneracy of HOMOs with amino groups.

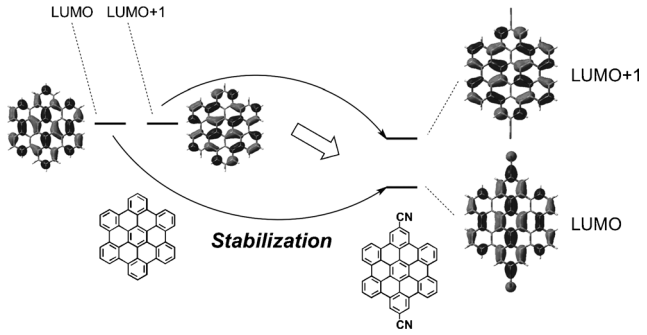

Figure 6. Splitting of LUMOs of unsubstituted HBC by cyano groups

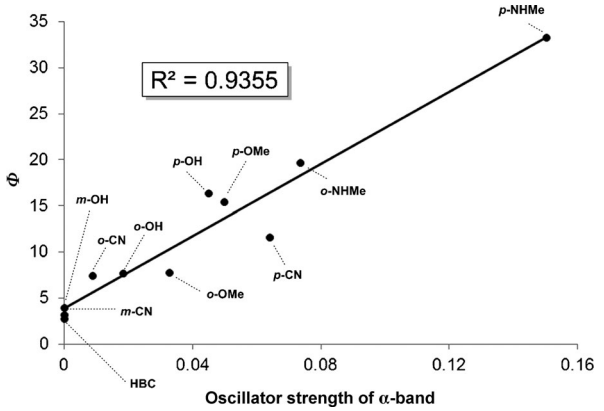

Figure 7. Correlation of the calculated oscillator strengths and observed fluorescence quantum yields of the α-band of various HBCs.

The solvents were removed under vacuum, and the crude product was purified by silica-gel column chromatography (CH_2Cl_2/*n*-hexane = 1:2) and recrystallized from CH_2Cl_2/MeOH to afford **5a** (18.7 mg, 0.018 mmol) in 89% yield as a yellow solid. ^{1}H NMR ($CDCl_3$, 500 MHz): δ = 9.02 (s, 4H), 9.00 (s, 4H), 8.71 (s, 4H), 7.14 (s, 8H), 4.24 (s, 6H), 2.46 (s, 12H), 2.25 ppm (s, 24H); ^{13}C NMR ($CDCl_3$, 126 MHz): δ = 158.8, 139.8, 139.2, 137.3, 136.4, 132.4, 131.0, 130.7, 128.4, 124.8, 123.6, 123.4, 120.8, 120.5, 108.2, 56.0, 21.3, 21.2 ppm; UV/Vis (CH_2Cl_2): λ_{max} (ε [$M^{-1}cm^{-1}$]) = 349 (82000), 365 (200000), 396 (58000), 444 (6500), 472 nm (10000); HR-MS (ESI-MS): *m/z* = 1055.4775, calcd for $(C_{80}H_{62}O_2)^+$ = 1055.4823 [$(M+H)^+$].

*2,11-Bis(3,3-dimethylbut-1-yn-1-yl)-5,8,14,17-tetramesitylhexabenzo[bc,ef,hi,kl,no,qr]coronene (**6a**)*

A flask containing **4a** (129 mg, 0.1 mmol), $[PdCl_2(PPh_3)_2]$ (2.11 mg, 3 mol%), and copper(I) iodide (1.14 mg, 6 mol%) was purged with N_2, and then charged with anhydrous and degassed THF (5 mL). Then, 1,8-diazabicyclo[5.4.0]undec-7-ene (91.3 mg, 6.0 equiv), pure water (2 drops), and 3,3-dimethylbut-1-yne (32.9 mg, 4.0 equiv) were added to this mixture at room temperature. The mixture was then stirred under room temperature for 18 h, quenched with aqueous HCl (1 M), extracted with CH_2Cl_2, and then dried over Na_2SO_4. The solvents were removed under vacuum, and the crude product was purified by silica-gel column chromatography (CH_2Cl_2/*n*-hexane = 1:2) and recrystallized from $CHCl_3$/MeOH to afford **6a** (113 mg, 0.097 mmol) in 97% yield as a yellow solid. ^{1}H NMR ($CDCl_3$, 500 MHz): δ = 9.21 (s, 4H), 9.06 (s, 4H), 9.01 (s, 4H), 7.13 (s, 8H), 2.46 (s, 12H), 2.24 (s, 24H), 1.47 ppm (s, 18H); ^{13}C NMR ($CDCl_3$, 126 MHz): δ = 140.2, 139.1, 137.3, 136.3, 130.9, 130.7, 130.4, 128.4, 125.4, 124.9, 124.5, 123.6, 123.5, 122.9, 121.4, 121.2, 99.9, 79.7, 31.2, 28.2, 21.3, 21.2 ppm; UV/Vis (Toluene): λ_{max} (ε [$M^{-1}cm^{-1}$]) = 352 (110000), 372 (260000), 399 (98000), 416 nm (32000); HR-MS (ESI-MS): *m/z* = 1155.5855, calcd for $(C_{90}H_{74})^+$ = 1155.5863 [$(M+H)^+$].

Table 2. Two-photon absorption cross-sections of **6**, **7**, and **8** in toluene.

Type	Compound	Functionality	σ [GM]
ortho	**6b**	*t*Bu-ethynyl	400
	7b	CN	420
	8b	NMes	440
meta	**6c**	*t*Bu-ethynyl	480
	7c	CN	690
para	**6a**	*t*Bu-ethynyl	700
	7a	CN	790
	8a	NMes	910

*N2,N11,5,8,14,17-Hexamesitylhexabenzo[bc,ef,hi,kl,no,qr]coronene-2,11-diamine (**7a**)*

A flask containing **4a** (258 mg, 0.2 mmol), $[Pd_2(dba)_3]$·$CHCl_3$ (10.4 mg, 5 mol%), 1,1′-bis(diphenylphosphino)ferrocene (11.1 mg, 10 mol%), and cesium carbonate (391 mg, 6.0 equiv) was purged with N_2, and then charged with anhydrous and degassed toluene (15 mL). 2,4,6-Trimethylaniline (216 mg, 8.0 equiv) was added to this mixture dropwise at room temperature. The mixture was then stirred under reflux for 24 h, quenched with CH_2Cl_2, and then the solvent was removed under vacuum. The crude product was purified by silica-gel column chromatography ($CHCl_3$/*n*-hexane = 1:3) and recrystallized from CH_2Cl_2/MeOH to afford **7a** (216 mg, 0.17 mmol) in 86% yield as a yellow solid. ^{1}H NMR ($CDCl_3$, 500 MHz): δ = 8.92 (s, 4H), 8.81 (s, 4H), 8.28 (s, 4H), 7.10 (s, 8H), 7.04 (s, 4H), 5.73 (s, 2H, NH), 2.44 (s, 12H), 2.38 (s, 6H), 2.34 (s, 12H), 2.22 ppm (s, 24H); ^{13}C NMR ($CDCl_3$, 126 MHz): δ = 145.6, 139.4, 139.2, 137.0, 136.4, 135.8, 135.6, 134.9, 132.1, 130.8, 130.6, 129.8, 128.4, 124.8, 123.4, 123.2, 120.7, 120.0, 119.3, 107.5, 21.3, 21.1, 18.6 ppm; UV/Vis (CH_2Cl_2): λ_{max} (ε [$M^{-1}cm^{-1}$]) = 327 (68000), 359 (72000), 377 (150000), 433 (24000), 459 (13000), 491 nm (14000); HR-MS (ESI-MS): *m/z* = 1260.6331, calcd for $(C_{96}H_{80}N_2)^+$ = 1260.6316 [$(M)^+$].

*5,8,14,17-Tetramesitylhexabenzo[bc,ef,hi,kl,no,qr]coronene-2,11-dicarbonitrile (**8a**)*

A flask containing **4a** (64.6 mg, 0.05 mmol), $[Pd_2(dba)_3]$·$CHCl_3$ (2.59 mg, 5 mol%), 1,1′-bis(diphenylphosphino)ferrocene (2.77 mg, 10 mol%), KCN (26.0 mg, 8.0 equiv), and zinc powder (0.19 mg, 6 mol%) was purged with N_2, and then charged with an anhydrous and degassed mixture of toluene/NMP = 1:1 (4 mL). The mixture was then stirred at 60 °C for 24 h, quenched with aqueous HCl (1 M), extracted with CH_2Cl_2, and then dried over Na_2SO_4. The solvents were removed under vacuum, and the crude product was purified by silica-gel column chromatography (CH_2Cl_2/*n*-hexane = 2:1) and recrystallized from CH_2Cl_2/MeOH to afford **8a** (37.5 mg, 0.036 mmol) in 72% yield as a yellow solid. ^{1}H NMR ($CDCl_3$, 500 MHz): δ = 9.44 (s, 4H), 9.11 (s, 4H), 9.08 (s, 4H), 7.14 (s, 8H), 2.46 (s, 12H), 2.24 ppm (s, 24H); ^{13}C NMR ($CDCl_3$, 126 MHz): δ = 141.1, 138.3, 137.6, 136.0, 131.8, 130.8, 129.5, 128.6, 127.9, 125.2, 124.9, 124.3, 124.0, 122.2, 121.2, 119.4, 111.2, 21.3, 21.2 ppm; UV/Vis (CH_2Cl_2): λ_{max} (ε [$M^{-1}cm^{-1}$]) = 353 (73000), 371 (180000), 402 (51000), 421 (20000),

449 (4900), 478 nm (5600); HR-MS (ESI-MS): $m/z = 1044.4451$, calcd for $(C_{78}H_{70})^+ = 1044.4438$ $[(M)^+]$.

1,2,3,4-Tetra(4-bromophenyl)-5,6-diphenylbenzene

A mixture of 2,3,4,5-tetrakis(4-bromophenyl)cyclopenta-2,4-dienone (3.10 g, 4.39 mmol) and 1,2-diphenylethyne (1.25 g, 1.6 equiv) in diphenyl ether (8 mL) was heated at 200 °C under N_2 for 36 h. The resulting mixture was cooled to room temperature and then diluted with diethyl ether. The precipitate was collected by filtration, washed with methanol and *n*-hexane, and dried to give 1,2,3,4-tetra(4-bromophenyl)-5,6-diphenylbenzene (3.47 g, 4.08 mmol) in 93% yield as a white solid. ^{1}H NMR ($CDCl_3$, 500 MHz): $\delta = 7.06$ (d, $J = 8.5$ Hz, 4H), 7.02 (d, $J = 8.5$ Hz, 4H), 6.85–6.90 (m, 6H), 6.72–6.78 (m, 4H), 6.66 (d, $J = 2.5$ Hz, 4H), 6.64 ppm (d, $J = 2.0$ Hz, 4H); ^{13}C NMR ($CDCl_3$, 126 MHz): $\delta = 141.0$, 139.7, 139.4, 138.94, 138.91, 138.8, 132.7, 131.1, 130.3, 130.1, 126.9, 125.7, 120.1, 119.9 ppm; HR-MS (ESI-MS): $m/z = 884.8457$, calcd for $(C_{42}H_{26}Br_4)^- = 884.8425$ $[(M+Cl)^-]$.

1,2,3,4-Tetra(4-mesitylphenyl)-5,6-diphenylbenzene

A flask containing 1,2,3,4-tetra(4-bromophenyl)-5,6-diphenylbenzene (2.56 g, 3.0 mmol), $[Pd_2(dba)_3]\cdot CHCl_3$ (82.4 mg, 3 mol%), and di-*tert*-butylphosphine oxide (29.2 mg, 6 mol%) was purged with N_2, and then charged with anhydrous and degassed THF (10 mL) and the mixture was stirred for 15 min. To this mixture was added dropwise a solution of mesitylmagnesium bromide prepared previously from mesityl bromide (4.78 g, 8.0 equiv) and magnesium (0.874 g, 12.0 equiv) in anhydrous degassed THF (30 mL) at room temperature. The mixture was then stirred at 60 °C for 48 h, quenched with aqueous HCl (1 M), extracted with CH_2Cl_2, and then dried over Na_2SO_4. The solvents were removed under vacuum, and the crude product was purified by silica-gel column chromatography ($CHCl_3$) and recrystallized from diethyl ether to afford **2** (2.83 g, 2.82 mmol) in 94% yield as a white solid. ^{1}H NMR ($CDCl_3$, 500 MHz): $\delta = 7.02$ (d, $J = 8.5$ Hz, 4H), 6.82–6.96 (m, 22H), 6.69 (d, $J = 8$ Hz, 4H), 6.64 (d, $J = 8.5$ Hz, 4H), 2.291 (s, 6H), 2.286 (s, 6H), 2.286 (s, 6H), 1.81 (s, 6H), 1.80 (s, 6H), 1.78 (s, 6H), 1.76 ppm (s, 6H); ^{13}C NMR ($CDCl_3$, 126 MHz): $\delta = 140.8$, 140.6, 140.5, 140.1, 139.2, 139.13, 139.06, 139.0, 137.9, 137.8, 136.23, 136.16, 135.95, 135.89, 135.6, 131.9, 131.7, 131.6, 127.75, 127.69, 127.5, 126.6, 125.1, 21.0, 20.4, 20.3 ppm; HR-MS (ESI-MS): $m/z = 1006.5502$, calcd for $(C_{78}H_{70})^+ = 1006.5472$ $[(M)^+]$.

*2,5,8,11-Tetramesitylhexabenzo[bc,ef,hi,kl,no,qr]coronene (**1b**)*

A solution of $FeCl_3$ (4.87 g, 20.0 equiv) in CH_3NO_2 (8 mL) was added to a stirred solution of 1,2,3,4-tetra(4-mesitylphenyl)-5,6-diphenylbenzene (1.51 g, 1.50 mmol) in anhydrous CH_2Cl_2/EtOH (150 mL:0.075 mL). The reaction mixture was stirred for 1 h with continuous N_2 bubbling through the reaction mixture. The mixture was poured into MeOH (100 mL) and concentrated with a rotary evaporator. The crude product was purified by silica-gel column chromatography (CH_2Cl_2/*n*-hexane = 1:2) and recrystallized from CH_2Cl_2/MeOH to afford **1b** (1.42 g, 1.43 mmol) in 95% yield as a yellow solid. This product was soluble enough in organic solvents such as CH_2Cl_2, $CHCl_3$, and toluene. ^{1}H NMR ($CDCl_3$, 500 MHz): $\delta = 9.06$ (s, 2H), 9.03 (s, 2H), 8.99 (s, 2H), 8.93 (s, 2H), 8.91 (d, $J = 8$ Hz, 2H), 8.77 (d, $J = 8$ Hz, 2H), 7.87 (t, $J = 8$ Hz, 2H), 7.13 (s, 4H), 7.12 (s, 4H), 2.48 (s, 6H), 2.45 (s, 6H), 2.29 (s, 12H), 2.25 ppm (s, 12H); ^{13}C NMR ($CDCl_3$, 500 MHz): $\delta = 139.9$, 139.7, 139.2, 139.1, 137.1, 136.3, 136.1, 131.0, 130.9, 130.8, 130.7, 130.2, 130.1, 128.42, 128.39, 126.6, 125.2, 124.5, 124.2, 123.5, 123.4, 123.3, 123.2, 121.9, 121.7, 121.1, 121.0, 21.35, 21.29, 21.19, 21.17 ppm; UV/Vis (CH_2Cl_2): λ_{max} (ε [$M^{-1}cm^{-1}$]) = 345 (90000), 361 (210000), 391 nm (71000); HR-MS (ESI-MS): $m/z = 995.4634$, calcd for $(C_{78}H_{58})^+ = 995.4611$ $[(M+H)^+]$.

*2,5-Diboryl-8,11,14,17-tetramesitylhexabenzo[bc,ef,hi,kl,no,qr]coronene (**2b**)*

A flask containing **1b** (1.19 g, 1.20 mmol), bis(pinacolato)diboron (1.22 g, 4.0 equiv), 4,4′-di-*tert*-butyl-2,2′-bipyridyl (19.3 mg, 6 mol%), and $[\{Ir(OMe)(cod)\}_2]$ (23.9 mg, 3 mol%) was purged with N_2, and then charged with degassed anhydrous mesitylene/*tert*-butyl methyl ether (20 mL:10 mL). The mixture was then stirred at 80 °C for 36 h. The crude product was purified by silica-gel column chromatography (CH_2Cl_2/*n*-hexane = 1:2) and recrystallized from CH_2Cl_2/MeOH to afford **2b** (1.32 g, 1.06 mmol) in 88% yield as a yellow solid. ^{1}H NMR ($CDCl_3$, 500 MHz): $\delta = 9.84$ (s, 2H), 9.69 (s, 2H), 9.24 (s, 2H), 9.01 (s, 2H), 9.00 (s, 2H), 8.99 (s, 2H), 7.16 (s, 4H), 7.08 (s, 4H), 2.48 (s, 6H), 2.42 (s, 6H), 2.25 (s, 12H), 2.23 (s, 12H), 1.57 ppm (s, 24H); ^{13}C NMR ($CDCl_3$, 126 MHz): $\delta = 140.1$, 140.0, 139.4, 139.0, 137.3, 137.1, 136.5, 136.1, 131.2, 131.0, 130.98, 130.86, 130.1, 129.6, 128.9, 128.8, 127.7, 124.42, 124.38, 123.52, 123.48, 123.1, 121.8, 121.7, 121.6, 84.4, 25.1, 21.31, 21.29, 21.19, 21.14 ppm; UV/Vis (CH_2Cl_2): λ_{max} (ε [$M^{-1}cm^{-1}$]) = 349 (100000), 366 (240000), 396 nm (83000); HR-MS (ESI-MS): $m/z = 1247.6294$, calcd for $(C_{90}H_{80}B_2O_4)^+ = 1247.6341$ $[(M+H)^+]$.

*8,11,14,17-Tetramesitylhexabenzo[bc,ef,hi,kl,no,qr]coronene-2,5-diol (**3b**)*

A flask containing **2b** (624 mg, 0.5 mmol) was purged with N_2, and then charged with a degassed mixture of THF/acetone/H_2O (30 mL:4 mL:2 mL). Oxone (1.23 g, 4.0 equiv) was then added to this mixture, which was then stirred at room temperature for 3 h. The flask was cooled to 0 °C (ice/water) and saturated aqueous sodium thiosulfate was added dropwise. The reaction mixture was diluted with CH_2Cl_2 and the organic layers were separated. The aqueous layer was extracted with CH_2Cl_2. The combined organic layers were dried over Na_2SO_4, and concentrated with a rotary evaporator. The crude product was purified by silica-gel column chromatography (CH_2Cl_2/ethyl acetate = 1:1) and recrystallized from CH_2Cl_2/*n*-hexane to afford **3b** (405 mg, 0.40 mmol) in 79% yield as a yellow solid. ^{1}H NMR ($CDCl_3$, 500 MHz): $\delta = 9.04$ (s, 2H), 9.01 (s, 2H), 8.99 (s, 2H), 8.78 (s, 2H), 8.31 (s, 2H), 8.01 (s, 2H), 7.10 (s, 8H), 5.27 (s, 2H, OH), 2.46 (s, 6H), 2.43 (s, 6H), 2.27 (s, 12H), 2.23 ppm (s, 12H); ^{13}C NMR ($CDCl_3$, 126 MHz): $\delta = 154.22$, 154.15, 139.7, 139.6, 139.0, 137.11, 137.08, 136.17, 136.09, 132.3. 132.2, 131.48, 131.38, 130.9, 130.7, 124.6, 124.5, 123.6, 123.4, 123.3, 120.5, 120.3, 120.2, 120.1, 120.0, 109.3, 109.0, 21.4, 21.3, 21.18, 21.15 ppm; UV/Vis (CH_2Cl_2): λ_{max} (ε [$M^{-1}cm^{-1}$]) = 348 (86000), 364 (210000), 395 nm (62000); HR-MS (ESI-MS): $m/z = 1027.4488$, calcd for $(C_{78}H_{58}O_2)^+ = 1027.4510$ $[(M+H)^+]$.

*8,11,14,17-Tetramesitylhexabenzo[bc,ef,hi,kl,no,qr]coronene-2,5-diyl bis(trifluoromethanesulfonate) (**4b**)*

A flask containing **3b** (103 mg, 0.1 mmol) was purged with N_2, and then charged with anhydrous and degassed CH_2Cl_2 (5 mL) and pyridine (0.062 mL, 8.0 equiv), then the mixture was stirred for 1 min. Trifluoromethanesulfonic anhydride (0.017 mL, 4.0 equiv) was added dropwise to this mixture at room temperature. The mixture was then stirred at room temperature for 3 h, quenched with aqueous HCl (1 M), extracted with CH_2Cl_2, and then dried over Na_2SO_4. The solvents were removed under vacuum, and the crude product was purified by silica-gel column chromatography (CH_2Cl_2/*n*-hexane = 1:2) and recrystallized from CH_2Cl_2/MeOH to afford **4b** (105 mg, 0.081 mmol) in 81% yield as a yellow solid. ^{1}H NMR ($CDCl_3$, 500 MHz): $\delta = 9.12$ (s, 2H), 9.08 (s, 2H), 9.07 (s, 2H), 8.99 (s, 2H), 8.96 (s, 2H), 8.78 (s, 2H), 7.17 (s, 4H), 7.11 (s, 4H), 2.49 (s, 6H), 2.44 (s, 6H), 2.26 (s, 12H), 2.25 ppm (s, 12H); ^{13}C NMR ($CDCl_3$, 126 MHz): $\delta = 148.5$, 140.9, 140.7, 138.7, 138.4, 137.6, 137.4, 136.2, 136.0, 133.4, 131.6, 131.2, 131.1, 130.8, 129.4, 128.6, 128.5, 125.2, 125.1, 124.4, 124.1, 123.9, 123.8, 122.1, 121.4, 120.3, 120.0, 117.7, 115.4, 114.5, 21.30, 21.28, 21.17 ppm; UV/Vis (CH_2Cl_2): λ_{max} (ε [$M^{-1}cm^{-1}$]) = 344 (110000), 360 (280000), 381 nm (87000); HR-MS (ESI-MS): $m/z = 1291.3526$, calcd for $(C_{80}H_{56}F_6O_6S_2)^+ = 1291.3495$ $[(M+H)^+]$.

*2,5,8,11-Tetramesityl-14,17-dimethoxyhexabenzo[bc,ef,hi,kl,no,qr]coronene (**5b**)*

A flask containing **3b** (103 mg, 0.1 mmol) and potassium carbonate (83 mg, 6.0 equiv) was purged with N_2, and then charged with an anhydrous and degassed mixture of THF/acetone = 3:1 (4 mL). Then, iodomethane (0.3 mL, excess) was added dropwise to this reaction mixture at room temperature. The mixture was then stirred at 60 °C for 24 h, quenched with aqueous HCl (1 M), extracted with CH_2Cl_2, and then dried over Na_2SO_4. The solvents were removed under vacuum, and the crude product was purified by silica-gel column chromatography (CH_2Cl_2/*n*-

hexane = 1:2) and recrystallized from CH_2Cl_2/MeOH to afford **5b** (79.5 mg, 0.075 mmol) in 75% yield as a yellow solid. ^{1}H NMR ($CDCl_3$, 500 MHz): δ = 9.00 (s, 6H), 8.94 (s, 2H), 8.55 (s, 2H), 8.39 (s, 2H), 7.14 (s, 4H), 7.09 (s, 4H), 4.13 (s, 6H), 2.47 (s, 6H), 2.42 (s, 6H), 2.25 (s, 12H), 2.24 ppm (s, 12H); ^{13}C NMR ($CDCl_3$, 126 MHz): δ = 158.5, 139.7, 139.6, 139.3, 139.1, 137.2, 137.1, 136.4, 136.1, 132.3, 131.9, 131.0, 130.81, 130.77, 130.6, 128.4, 124.7, 124.6, 123.5, 123.4, 123.2, 120.7, 120.5, 120.3, 108.6, 107.3, 55.8, 21.3, 21.2 ppm; UV/Vis (CH_2Cl_2): λ_{max} (ε [$M^{-1}cm^{-1}$]) = 349 (91000), 366 (220000), 396 nm (64000); HR-MS (ESI-MS): *m/z* = 1055.4817, calcd for $(C_{80}H_{62}O_2)^+$ = 1055.4823 [$(M+H)^+$].

*2,5-Bis(3,3-dimethylbut-1-yn-1-yl)-8,11,14,17-tetramesitylhexabenzo[bc,ef,hi,kl,no,qr]coronene (**6b**)*

A flask containing **4b** (129 mg, 0.1 mmol), [$PdCl_2(PPh)_2$] (2.11 mg, 3 mol%), and copper(I) iodide (1.14 mg, 6 mol%) was purged with N_2, and then charged with anhydrous and degassed THF (5 mL). 1,8-Diazabicyclo[5.4.0]undec-7-ene (91.3 mg, 6.0 equiv), distilled water (3 drops), and 3,3-dimethylbut-1-yne (32.9 mg, 4.0 equiv) were added to this mixture at room temperature. The mixture was then stirred under room temperature for 18 h, quenched with aqueous HCl (1 M), extracted with CH_2Cl_2, and then dried over Na_2SO_4. The solvents were removed under vacuum, and the crude product was purified by silica-gel column chromatography (CH_2Cl_2/*n*-hexane = 1:2) and recrystallized from CH_2Cl_2/MeOH to afford **6b** (106 mg, 0.091 mmol) in 91% yield as a yellow solid. ^{1}H NMR ($CDCl_3$, 500 MHz): δ = 9.27 (s, 2H), 9.23 (s, 2H), 9.05 (s, 2H), 8.99 (s, 6H), 7.13 (s, 4H), 7.05 (s, 4H), 2.46 (s, 6H), 2.42 (s, 6H), 2.23 (s, 12H), 2.21 (s, 12H), 1.52 ppm (s, 18H); ^{13}C NMR ($CDCl_3$, 126 MHz): δ = 140.1, 139.1, 137.1, 136.3, 136.1, 130.9, 128.4, 125.7, 125.2, 124.3, 123.6, 121.4, 31.2, 28.2, 21.24, 21.17 ppm; UV/Vis (toluene): λ_{max} (ε [$D^{-1}cm^{-1}$]) = 336 (40000), 352 (120000), 370 (290000), 399 nm (120000); HR-MS (ESI-MS): *m/z* = 1155.5813, calcd for $(C_{90}H_{74})^+$ = 1155.5863 [$(M+H)^+$].

*N2,N5,8,11,14,17-Hexamesitylhexabenzo[bc,ef,hi,kl,no,qr]coronene-2,5-diamine (**7b**)*

A flask containing **4b** (129 mg, 0.1 mmol), [$Pd_2(dba)_3$]·$CHCl_3$ (3.1 mg, 3 mol%), 2,2′-bis(diphenylphosphino)-1,1′-binaphthyl (3.7 mg, 6 mol%), and cesium carbonate (195 mg, 6.0 equiv) was purged with N_2, and then charged with anhydrous and degassed toluene (12 mL). 2,4,6-Trimethylaniline (108 mg, 8.0 equiv) was added dropwise to this mixture at room temperature. The mixture was then stirred under reflux for 24 h, quenched with CH_2Cl_2, and then the solvents were removed under vacuum. The crude product was purified by silica-gel column chromatography ($CHCl_3$/*n*-hexane = 1:3) and recrystallization from CH_2Cl_2/MeOH to afford **7b** (108 mg, 0.086 mmol) in 86% yield as a yellow solid. ^{1}H NMR ($CDCl_3$, 500 MHz): δ = 8.978 (s, 2H), 8.974 (s, 2H), 8.965 (s, 2H), 8.89 (s, 2H), 8.39 (s, 2H), 7.88 (s, 2H), 7.12 (s, 4H), 7.09 (s, 2H), 7.01 (s, 4H), 5.69 (s, 2H, NH), 2.46 (s, 4H), 2.43 (s, 12H), 2.30 (s, 12H), 2.25 (s, 12H), 2.24 ppm (s, 12H); ^{13}C NMR ($CDCl_3$, 126 MHz): δ = 145.5, 139.4, 139.30, 139.27, 139.20, 137.05, 136.95, 136.4, 136.1, 135.6, 135.4, 135.1, 132.2, 132.0, 130.9, 130.7, 130.6, 129.5, 128.35, 128.33, 124.83, 124.75, 123.4, 123.29, 123.27, 123.18, 120.5, 120.1, 119.9, 119.3, 108.1, 106.8, 21.31, 21.29, 21.1, 18.5 ppm; UV/Vis (CH_2Cl_2): λ_{max} (ε [$M^{-1}cm^{-1}$]) = 330 (47000), 382 (140000), 455 (8700), 486 nm (7900); HR-MS (ESI-MS): *m/z* = 1260.6293, calcd for $(C_{96}H_{80}N_2)^+$ = 1260.6316 [$(M+H)^+$].

*8,11,14,17-Tetramesitylhexabenzo[bc,ef,hi,kl,no,qr]coronene-2,5-dicarbonitrile (**8b**)*

A flask containing **4b** (129 mg, 0.1 mmol), [$Pd_2(dba)_3$]·$CHCl_3$ (3.1 mg, 3 mol%), 1,1′-bis(diphenylphosphino)ferrocene (3.3 mg, 6 mol%), KCN (52.0 mg, 8.0 equiv), and zinc powder (0.39 mg, 6 mol%) was purged with N_2, and then charged with an anhydrous and degassed mixture of toluene/NMP = 1:1 (5 mL). The mixture was then stirred at 100 °C for 24 h, quenched with aqueous HCl (1 M), extracted with CH_2Cl_2, and then dried over Na_2SO_4. The solvents were removed under vacuum, and the crude product was purified by silica-gel column chromatography ($CHCl_3$/*n*-hexane = 2:1) and recrystallized from $CHCl_3$/*n*-hexane to afford **8b** (75.1 mg, 0.072 mmol) in 72% yield as a yellow solid. ^{1}H NMR ($CDCl_3$, 500 MHz): δ = 9.17 (s, 2H), 9.13 (s, 4H), 8.73 (s, 2H), 8.69 (s, 2H), 8.22 (s, 2H), 7.12 (s, 8H), 2.50 (s, 6H), 2.45 (s, 6H), 2.31 (s, 12H), 2.26 ppm (s, 12H); ^{13}C NMR ($CDCl_3$, 126 MHz): δ = 141.5, 140.9, 138.6, 138.1, 137.5, 137.4, 136.1, 135.8, 131.0, 130.9, 130.8, 130.5, 128.6, 128.5, 126.8, 125.3, 124.9, 124.40, 124.37, 123.64, 123.57, 123.4, 123.3, 121.4, 119.6, 118.4, 110.1, 21.4, 21.3 ppm; UV/Vis (CH_2Cl_2): λ_{max} (ε [$M^{-1}cm^{-1}$]) = 352 (73000), 370 (150000), 410 (40000), 448 nm (3000); HR-MS (ESI-MS): *m/z* = 1045.4489, calcd for $(C_{78}H_{70})^+$ = 1045.4516 [$(M+H)^+$].

*5,11,17-Trimesitylhexabenzo[bc,ef,hi,kl,no,qr]coronene-2,8,14-triyl tris(trifluoromethanesulfonate) (**4c**)*

A flask containing **3c** (92.5 mg, 0.1 mmol) was purged with N_2, and then charged with anhydrous and degassed CH_2Cl_2 (5 mL) and pyridine (0.064 mL, 8.0 equiv). Then, trifluoromethanesulfonic anhydride (0.11 mL, 6.0 equiv) was added dropwise to this mixture at room temperature. The mixture was then stirred at room temperature for 16 h, quenched with aqueous HCl (1 M), extracted with CH_2Cl_2, and then dried over Na_2SO_4. The solvents were removed under vacuum, and the crude product was purified by silica-gel column chromatography (CH_2Cl_2/*n*-hexane = 1:2) and recrystallized from CH_2Cl_2/MeOH to afford **4c** (94.5 mg, 0.072 mmol) in 72% yield as a yellow solid. ^{1}H NMR ($CDCl_3$, 500 MHz): δ = 9.08 (s, 6H), 9.06 (s, 6H), 7.24 (s, 6H), 2.53 (s, 9H), 2.29 ppm (s, 18H); ^{13}C NMR ($CDCl_3$, 126 MHz): δ = 148.9, 141.2, 138.2, 138.1, 136.4, 133.1, 130.0, 128.7, 125.1, 125.0, 124.6, 121.9, 120.8, 120.3, 117.7, 115.0, 21.3, 21.2 ppm; UV/Vis (CH_2Cl_2): λ_{max} (ε [$D^{-1}cm^{-1}$]) = 329 (30000), 344 (80000), 361 (190000), 391 nm (64000); HR-MS (ESI-MS): *m/z* = 1321.2186, calcd for $(C_{72}H_{45}F_9O_9S_3)^+$ = 1321.2155 [$(M+H)^+$].

*2,8,14-Tris(3,3-dimethylbut-1-yn-1-yl)-5,11,17-trimesitylhexabenzo[bc,ef,hi,kl,no,qr]coronene (**6c**)*

A flask containing **4c** (132 mg, 0.1 mmol), [$PdCl_2(PPh)_2$] (3.5 mg, 5 mol%), and copper(I) iodide (1.9 mg, 10 mol%) was purged with N_2, and then charged with anhydrous and degassed THF (10 mL). 1,8-Diazabicyclo[5.4.0]undec-7-ene (91.3 mg, 6.0 equiv), distilled water (2 drops), and 3,3-dimethylbut-1-yne (49.3 mg, 6.0 equiv) were added to this mixture at room temperature. The mixture was then stirred at room temperature for 24 h, quenched with aqueous HCl (1 M), extracted with CH_2Cl_2, and then dried over Na_2SO_4. The solvents were removed under vacuum, and the crude product was purified by silica-gel column chromatography (toluene/*n*-hexane = 1:8) and recrystallized from CH_2Cl_2/MeOH to afford **6c** (95.0 mg, 0.085 mmol) in 85% yield as a yellow solid. ^{1}H NMR ($CDCl_3$, 500 MHz): δ = 9.19 (s, 6H), 9.05 (s, 6H), 7.18 (s, 6H), 2.49 (s, 9H), 2.26 (s, 18H), 1.47 ppm (s, 27H); ^{13}C NMR ($CDCl_3$, 126 MHz): δ = 140.4, 139.5, 137.7, 136.7, 130.8, 130.7, 128.7, 125.6, 125.0, 124.7, 123.8, 123.1, 121.9, 121.3, 100.1, 80.0, 31.5, 31.4, 28.5, 21.5 ppm; UV/Vis (CH_2Cl_2); λ_{max} (ε [$M^{-1}cm^{-1}$]) = 354 (100000), 372 (270000), 401 nm (120000); HR-MS (ESI-MS): *m/z* = 1117.5751, calcd for $(C_{87}H_{72})^+$ = 1117.5707 [$(M+H)^+$].

*5,11,17-Trimesitylhexabenzo[bc,ef,hi,kl,no,qr]coronene-2,8,14-tricarbonitrile (**8c**)*

A flask containing **4c** (26.4 mg, 0.02 mmol), [$Pd_2(dba)_3$]·$CHCl_3$ (1.04 mg, 5 mol%), 1,1′-bis(diphenylphosphino)ferrocene (1.11 mg, 10 mol%), KCN (15.6 mg, 12.0 equiv), and zinc powder (0.078 mg, 6 mol%) was purged with N_2, and then charged with anhydrous and degassed toluene/NMP = 1:1 (2 mL). The mixture was then stirred at 60 °C for 24 h, quenched with aqueous HCl (1 M), extracted with CH_2Cl_2, and then dried over Na_2SO_4. The solvents were removed under vacuum, and the crude product was purified by silica-gel column chromatography (CH_2Cl_2/*n*-hexane = 1:1) and recrystallized from CH_2Cl_2/MeOH to afford **8c** (10.6 mg, 0.011 mmol) in 56% yield as a yellow solid. ^{1}H NMR ($CDCl_3$, 500 MHz): δ = 9.46 (s, 6H), 9.15 (s, 6H), 7.19 (s, 6H), 2.49 (s, 9H), 2.26 ppm; ^{13}C NMR ($CDCl_3$, 126 MHz): δ = 142.0, 138.0, 137.9, 136.0, 131.3, 129.8, 128.7, 127.6, 125.5, 125.0, 124.3, 123.8, 120.4, 119.2, 111.5, 21.3, 21.2 ppm; UV/Vis (CH_2Cl_2): λ_{max} (ε [$M^{-1}cm^{-1}$]) = 329 (30000), 344 (80000), 368 (190000), 391 nm (64000); HR-MS (ESI-MS): *m/z* = 952.3667, calcd for $(C_{72}H_{45}N_3)^+$ = 952.3686 [$(M+H)^+$].

Two-Photon Absorption Experiments

The two-photon absorption (TPA) spectrum was measured in the NIR region using the open-aperture Z-scan method with 130 fs pulses from an optical parametric amplifier (Light Conversion, TOPAS) operating at a repetition rate of 2 kHz generated from a Ti:sapphire regenerative amplifier system (Spectra-Physics, Hurricane). After passing through a 10 cm focal length lens, the laser beam was focused and passed through a 1 mm quartz cell. As the position of the sample cell could be controlled along the laser beam direction (z axis) using the motorcontrolled delay stage, the local power density within the sample cell could be simply controlled under constant laser intensity. The transmitted laser beam from the sample cell was then detected by the same photodiode as used for reference monitoring. The on-axis peak intensity of the incident pulses at the focal point, I_0, ranged from 40 to 60 GW cm^{-2}. For a Gaussian beam profile, the nonlinear absorption coefficient can be obtained by curve fitting of the observed open-aperture traces $T(z)$, as shown by Equation (1):

$$T(z) = 1 - \frac{\beta I_0 (1 - e^{-\alpha_0 l})}{2\alpha_0 [1 + (z/z_0)^2]} \quad (1)$$

where α_0 is the linear absorption coefficient, l the sample length, and z_0 the diffraction length of the incident beam. After the nonlinear absorption coefficient has been obtained, the TPA cross section $\sigma^{(2)}$ of one solute molecule (in units of GM, where 1 GM = 10^{-50} cm^4 s photon^{-1} molecule^{-1}) can be determined by using the following relationship, as shown in Equation (2):

$$\beta = \frac{10^{-3} \sigma^{(2)} N_A d}{h\nu} \quad (2)$$

where N_A is the Avogadro constant, d is the concentration of the compound in solution, h is the Planck constant, and ν is the frequency of the incident laser beam.

Acknowledgements

This work was supported by Grants-in-Aid for Scientific Research (Nos. 22750036 and 23108705 "pi-Space") from MEXT, Japan. H.S. also acknowledges Daiko Foundation for financial support. The work at Yonsei University was supported by the Midcareer Researcher Program (2010-0029668), an AFSOR/APARD grant (no. FA2386-09-1-4092) and World Class University (R32-2010-000-10217) Programs of the Ministry of Education, Science, and Technology (MEST) of Korea.

[1] a) *Carbon-Rich Compounds* (Eds.: M. M. Haley, R. R. Tykwinski), Wiley-VCH, Weinheim, **2006**; b) R. G. Harvey, *Polycyclic Aromatic Hydrocarbons*, Wiley-VCH, Weinheim, **1997**; c) *Functional Organic Materials* (Eds.: T. J. J. Müller, U. H. F. Bunz), Wiley-VCH, Weinheim, **2007**.

[2] a) J. E. Anthony, *Angew. Chem.* **2008**, *120*, 460; *Angew. Chem. Int. Ed.* **2008**, *47*, 452; b) T. M. Figueira-Duarte, K. Müllen, *Chem. Rev.* **2011**, *111*, 7260; c) F. Würthner, *Chem. Commun.* **2004**, 1564; d) X. Feng, W. Pisula, K. Müllen, *Pure. Appl. Chem.* **2009**, *81*, 2203.

[3] Recent achievements of polycyclic aromatic hydrocarbons, see: a) L. T. Scott, E. A. Jackson, Q. Zhang, B. D. Steinberg, M. Bancu, B. Li, *J. Am. Chem. Soc.* **2012**, *134*, 107; b) A. Konishi, Y. Hirao, M. Nakano, A. Shimizu, E. Botek, B. Champagne, D. Shiomi, K. Sato, T. Takui, K. Matsumoto, H. Kurata, T. Kubo, *J. Am. Chem. Soc.* **2010**, *132*, 11021; c) L. Dössel, L. Gherghel, X. Feng, K. Müllen, *Angew. Chem.* **2011**, *123*, 2588; *Angew. Chem. Int. Ed.* **2011**, *50*, 2540; d) S. Hitosugi, W. Nakanishi, T. Yamasaki, H. Isobe, *Nat. Commun.* **2011**, *2*, 492; e) M. Watanabe, Y. J. Chang, S.-W. Liu, T.-H. Chao, K. Goto, M. M. Islam, C.-H. Yuan, Y.-T. Tao, Y. Shinmyozu, T. J. Chow, *Nat. Chem.* **2012**, *4*, 574; f) B. Purushothaman, M. Bruzek, S. R. Parkin, A.-F. Miller, J. E. Anthony, *Angew. Chem.* **2011**, *123*, 7151; *Angew. Chem. Int. Ed.* **2011**, *50*, 7013.

[4] a) J. P. Hill, W. Jin, A. Kosaka, T. Fukushima, H. Ichihara, T. Shimomura, K. Ito, T. Hashizume, N. Ishii, T. Aida, *Science* **2004**, *304*, 1481; b) S. Xiao, M. Myers, Q. Miao, S. Sanaur, K. Pang, M. L. Steigerwald, C. Nuckolls, *Angew. Chem.* **2005**, *117*, 7556; *Angew. Chem. Int. Ed.* **2005**, *44*, 7390.

[5] a) X. Yang, X. Dou, K. Müllen, *Chem. Asian J.* **2008**, *3*, 759; b) J. Wu, M. D. Watson, K. Müllen, *Angew. Chem.* **2003**, *115*, 5487; *Angew. Chem. Int. Ed.* **2003**, *42*, 5329; c) S. Ito, M. Wehmeier, J. D. Brand, C. Kübel, R. Epsch, J. P. Rabe, K. Müllen, *Chem. Eur. J.* **2000**, *6*, 4327.

[6] a) W. Pisula, X. Feng, K. Müllen, *Adv. Mater.* **2010**, *22*, 3634; b) J. Wu, W. Pisula, K. Müllen, *Chem. Rev.* **2007**, *107*, 718.

[7] a) X. Feng, W. Pisula, M. Takase, X. Dou, V. Enkelmann, M. Wagner, N. Ding, K. Müllen, *Chem. Mater.* **2008**, *20*, 2872; b) J. Wu, M. Baumgarten, M. G. Debije, J. M. Warman, K. Müllen, *Angew. Chem.* **2004**, *116*, 5445; *Angew. Chem. Int. Ed.* **2004**, *43*, 5331; c) L. Chen, X. Dou, W. Pisula, X. Yang, D. Wu, G. Floudas, X. Feng, K. Müllen, *Chem. Commun.* **2012**, *48*, 702.

[8] M. Kastler, W. Pisula, D. Wasserfallen, T. Pakula, K. Müllen, *J. Am. Chem. Soc.* **2005**, *127*, 4286.

[9] a) W. W. H. Wong, D. Vak, Th. B. Singh, S. Ren, C. Yan, D. J. Jones, I. I. Liaw, R. N. Lamb, A. B. Holmes, *Org. Lett.* **2010**, *12*, 5000; b) W. W. H. Wong, T. B. Singh, D. Vak, W. Pisula, C. Yan, X. Feng, E. L. Williams, K. L. Chan, Q. Mao, D. J. Jones, C.-Q. Ma, K. Müllen, P. Bäuerle, A. B. Holmes, *Adv. Funct. Mater.* **2010**, *20*, 927.

[10] a) S. K. Sadhukhan, C. Viala, A. Gourdon, *Synthesis* **2003**, 1521; b) P. T. Herwig, V. Enkelmann, O. Schmelz, K. Müllen, *Chem. Eur. J.* **2000**, *6*, 1834.

[11] a) T. Teraoka, S. Hiroto, H. Shinokubo, *Org. Lett.* **2011**, *13*, 2532; b) R. Yamaguchi, S. Hiroto, H. Shinokubo, *Org. Lett.* **2012**, *14*, 2472.

[12] a) I. A. I. Mkhalid, J. H. Barnard, T. D. Marder, J. M. Mulphy, J. F. Hartwig, *Chem. Rev.* **2010**, *110*, 890; b) N. Miyaura, *Bull. Chem. Soc. Jpn.* **2008**, *81*, 1535; c) T. Ishiyama, N. Miyaura, *J. Organomet. Chem.* **2003**, *680*, 3.

[13] a) D. N. Coventry, A. S. Basanov, A. E. Goeta, J. A. K. Howard, T. B. Marder, R. N. Perutz, *Chem. Commun.* **2005**, 2172; b) H. Hata, H. Shinokubo, A. Osuka, *J. Am. Chem. Soc.* **2005**, *127*, 8264; c) S. Hiroto, I. Hisaki, H. Shinokubo, A. Osuka, *Angew. Chem.* **2005**, *117*, 6921; *Angew. Chem. Int. Ed.* **2005**, *44*, 6763; d) T. Kimoto, K. Tanaka, Y. Sakai, A. Ohno, K. Yoza, K. Kobayashi, *Org. Lett.* **2009**, *11*, 3658; e) R. Ozawa, K. Yoza, K. Kobayashi, *Chem. Lett.* **2011**, *40*, 941; f) A. G. Crawford, Z. Liu, I. A. I. Mkhalid, M.-H. Thibault, N. Schwarz, G. Alcaraz, A. Steffen, J. C. Collings, A. S. Batsanov, J. A. K. Howard, T. B. Marder, *Chem. Eur. J.* **2012**, *18*, 5022; g) S. Hitosugi, Y. Nakamura, T. Matsuno, W. Nakanishi, H. Isobe, *Tetrahedron Lett.* **2012**, *53*, 1180.

[14] Crystallographic data for **3b**: $C_{80}H_{60}O_2Cl_6$, M_w = 1265.98, Monoclinic, Space Group = $P2_1/n$ a = 8.099(4) Å, b = 22.002(11) Å, c = 35.641(18) Å, β = 92.477(10)°, Z = 4, R = 0.0704 ($I > 2.0\sigma(I)$), R_w = 0.2471 (all data), GOF = 1.050. CCDC 894808 contains the supplementary crystallographic data for this paper. These data can be obtained free of charge from The Cambridge Crystallographic Data Centre via www.ccdc.cam.ac.uk/data_request/cif..

[15] X. Feng, J. Wu, V. Enkelmann, K. Müllen, *Org. Lett.* **2006**, *8*, 1145.

[16] a) G. Battagliarin, Y. Zhao, C. Li, K. Müllen, *Org. Lett.* **2011**, *13*, 3399; b) G. Battagliarin, C. Li, V. Enkelmann, K. Müllen, *Org. Lett.* **2011**, *13*, 3012; c) J. M. Murphy, X. Liao, J. F. Hartwig, *J. Am. Chem. Soc.* **2007**, *129*, 15434.

[17] D. S. Surry, S. L. Buchwald, *Chem. Sci.* **2011**, *2*, 27.

[18] a) K. Takagi, Y. Sakakibara, *Chem. Lett.* **1989**, 1957; b) R. Chidambaram, *Tetrahedron Lett.* **2004**, *45*, 1441.

[19] M. Kastler, J. Schmidt, W. Pisula, D. Sebastiani, K. Müllen, *J. Am. Chem. Soc.* **2006**, *128*, 9526.

[20] a) A. D. Becke, *Phys. Rev. A* **1988**, *38*, 3098; b) C. Lee, W. Yang, R. G. Parr, *Phys. Rev. B* **1988**, *37*, 785.

[21] A. G. Crawford, A. D. Dwyer, Z. Liu, A. Steffen, A. Beeby, L.-O. Pålsson, D. J. Tozer, T. B. Marder, *J. Am. Chem. Soc.* **2011**, *133*, 13349.

[22] Z. Zeng, Z. Guan, Q.-H. Xu, J. Wu, *Chem. Eur. J.* **2011**, *17*, 3837.

Received: August 7, 2012
Published online: October 24, 2012

